Available online at www.sciencedirect.com
ScienceDirect
Trans. Nonferrous Met. Soc. China 21(2011) 2378−2383
Transactions of Nonferrous Metals Society of China
www.tnmsc.cn

Effect of stannum addition on microstructure of as-cast and as-extruded Mg−5Li alloys

JIANG Bin[1, 2], YIN Heng-mei[1], YANG Qing-shan[1, 2], LI Rui-hong[1, 2], PAN Fu-sheng[1, 2]

1. College of Materials Science and Engineering, Chongqing University, Chongqing 400044, China;
2. National Engineering Research Center for Magnesium Alloys, Chongqing 400044, China

Received 10 November 2010; accepted 11 April 2011

Abstract: Mg−5Li−*x*Sn (*x*=0.15, 0.25 and 0.65, mass fraction) alloys were prepared. The microstructures of these alloys were investigated through optical microscope (OM), scanning electron microscope (SEM), X-ray diffractometer (XRD) and energy dispersive spectrometer (EDS). The results indicate that Sn additions produce a strong grain refinement effect on Mg−5Li alloy. The mean grain size of as-cast Mg−Li alloys with Sn is reduced remarkably from 556 μm to 345 μm, and that of the as-extruded alloys is reduced from 33 μm to 23 μm when the Sn content increases from 0.15% to 0.65%. The near net-like Mg_2Sn phase in the as-cast alloys is verified at the grain boundaries. After extrusion, the granular Mg_2Sn phase mainly exists inside the grains and thus can act as nucleation sites of *α*-Mg grains during the dynamic recrystallization and make the microstructure finer.

Key words: Mg−Li alloys; grain refinement; intermetallic compound; Sn

1 Introduction

Mg−Li alloys are the lightest magnesium alloy and have excellent plasticity [1−2]. Therefore, Mg−Li alloys can meet the light-weight demand in the applications of aircraft, aerospace and military, etc [3−4]. Lithium in Mg−Li alloys is a key factor affecting the property and microstructure. When the lithium content in Mg−Li alloy increases, the microstructure of the alloy will change from *α*-Mg (HCP)+*β*-Li (BBC) to *β*-Li (BBC) [5−6], a Mg−Li solid solution in Li structure and BCC structure. However, the strength of Mg−Li alloys containing *β*-Li phase is relatively low because of the soft *β*-Li phase, which has confined their application fields [6−7]. Although composite reinforcement can increase the strength [8−9], the lightness and ductility have to be sacrificed. Like AZ31 [10] and ZK60 [11] with *α*-Mg structure, Mg−5Li alloy has the same structure of *α*-Mg and has higher strength than the alloy of *β*-Li structure. It is notable that *α*-Mg phase with Li content has better plasticity due to the decrease of *c*/*a* value [12]. In order to coordinate high strength and good plasticity of the Mg−Li alloys, Mg−5Li alloy with a single *α*-Mg phase was chosen as an experimental alloy.

However, the as-cast Mg−Li alloy is generally prepared by common mould casting because of no usable semi-continuous casting technique and equipment due to the high chemical activity. Thus, the as-cast Mg−Li alloy has coarser grains. Many research results indicated that rapid solidification [13] and adding alloying element Al or Zn [14−15] can refine the grains. But, the rapid solidification processing is costly for mass production and the metastable Li_2MgAl or LiMgZn will be formed in Mg−Li−Al/Zn alloy and will resolve at 66 °C or even at room temperature [14], resulting in over-aging of Mg−Li−Al/Zn alloy [14−15]. Therefore, new grain refinement approaches need to be developed. There are a lot of researches related to the effect of Ce on Mg−8Li alloy [16], Mn on Mg−9Li alloy [17] and Y on Mg−7Li alloy [18], and these alloys are the dual phase structure of *α*-Mg+*β*-Li. Moreover, the effects of Sn on Mg [19], Mg−Zn−Al [20] and Mg−5Li−3Al−2Zn [21] were successfully presented for its potential properties. Hence, in this work, Mg−5Li−*x*Sn (*x*=0.15, 0.25 and 0.65, mass fraction) alloys with *α*-Mg structure were prepared to examine the effect of Sn on microstructure of Mg−5Li alloy for the first time.

Foundation item: Projects (51171212, 50725413) supported by the National Natural Science Foundation of China; Project (2007CB613706) supported by the National Basic Research Program of China; Project (2009AA03Z507) supported by the National High-tech Research Program of China; Projects (2010CSTC-BJLKR, CSTC2010AA4048) supported by Chongqing Science and Technology Commission, China
Corresponding author: JIANG Bin; Tel: +86-23-65111140; E-mail: jiangbinrong@cqu.edu.cn
DOI: 10.1016/S1003-6326(11)61023-6

2 Experimental

The materials used in this work were pure magnesium, pure lithium and pure stannum with purity of 99.9%. These materials were mixed together into a stainless steel crucible with nominal composition listed in Table 1, and then the crucible was put into an induction furnace. After the furnace chamber was pumped to a vacuum state, pure argon was put into the chamber as a protective gas. Subsequently, the experiment materials were heated to 700 °C until the alloy was completely melted, and the alloy melt was isothermally held for 10 min under the argon atmosphere. Finally, the alloys were cooled under the argon atmosphere and a cast ingot (85 mm in diameter and 150 mm in height) was obtained. The actual chemical compositions of the obtained ingots were determined with inductively coupled plasma atomic emission spectroscopy (ICP-AES). The result is shown in Table 1.

Table 1 Chemical composition of experimental alloys (mass fraction, %)

Alloy No.	Nominal	Actual
1	Mg−5Li−0.2Sn	Mg−5.06Li−0.15Sn
2	Mg−5Li−0.3Sn	Mg−4.87Li−0.25Sn
3	Mg−5Li−0.7Sn	Mg−4.97Li−0.65Sn

The extrusion was done at 250 °C and the extrusion ratio was 27. The bars of 16 mm in diameter were obtained after extrusion. The samples used for microstructure observation were cut from the same position. Microstructure was observed using optical microscopy and scanning electron microscopy (SEM, TESCAN VEGA). Before observation, the samples were polished and etched with an etchant of 4.0% (volume fraction) natal. The grain size was measured by the linear intercept method at the centre of transverse sections. The phase in the alloys was identified by Rigaku D/max 2500PC using Cu K_α radiation (λ=1.541 8 Å) operating at 4 (°)/min in the 2θ range of 10°−90°.

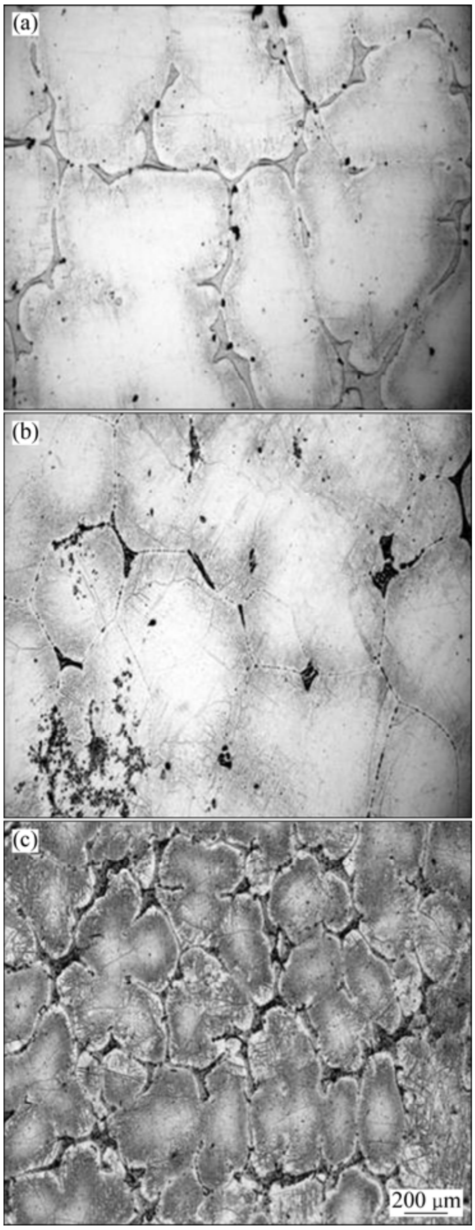

Fig. 1 Microstructures of as-cast Mg−5.06Li−0.15Sn (a), Mg−4.87Li−0.25Sn (b) and Mg−4.97Li−0.65Sn (c)

3 Results and discussions

3.1 Grain size of Mg−5Li alloys containing various Sn additions

Figure 1 shows the optical microstructures of as-cast Mg−5Li alloys with various Sn additions. Equiaxed grains are obtained, and granular and near net-like intermetallic compounds are observed. Notable grain refinement occurs at the addition of 0.65% Sn, in which the grain size reduces to 345 μm from 556 μm, as shown in Figs. 1(a) and (c). Although the grain refinement efficiency of the addition of Sn in the present Mg−5Li alloy is not as significant as that in Mg−Al alloys [20−21], the reduction of grain size is still remarkable.

The microstructures of as-extruded Mg−5Li−xSn (x=0.15, 0.25, 0.65) alloys are shown in Fig. 2. They are finer than those of the as-cast Mg−5Li−xSn alloys. The size of the as-extruded grains is reduced from 33 μm to 23 μm when the addition of Sn changes from 0.15% to 0.25%, as shown in Fig. 3, and becomes stable when the addition of Sn is 0.65%, which demonstrates that the addition of Sn into Mg−5Li alloys has a limited grain refinement effect. This agrees with the effect of addition of Al−5Ti−1B master alloy on the grain refinement of LA141 alloy [2].

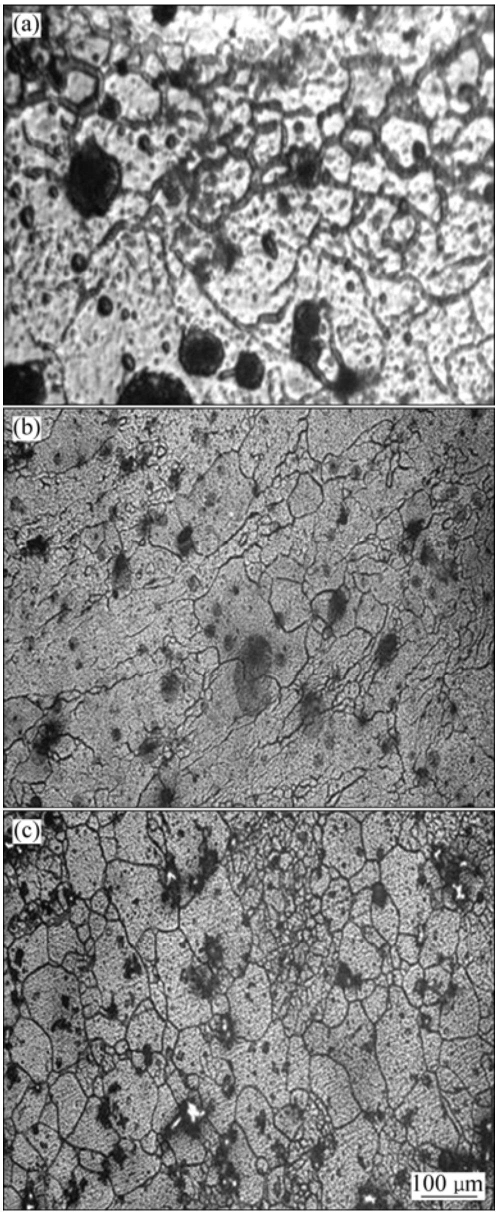

Fig. 2 Microstructures of as-extruded Mg−5.06Li−0.15Sn (a), Mg−4.87Li−0.25Sn (b) and Mg−4.97Li−0.65Sn (c) alloys

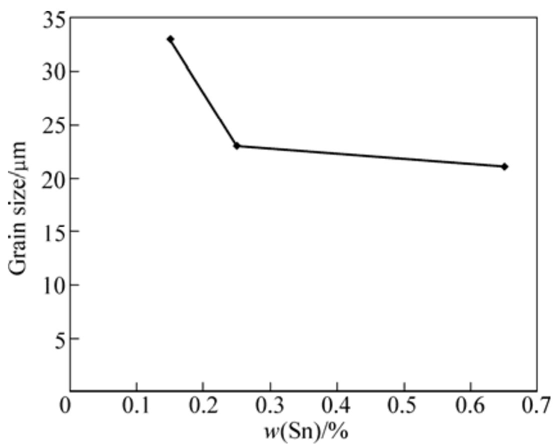

Fig. 3 Variation of grain size of as-extruded Mg−5Li with addition of Sn

3.2 Characteristics of intermetallic compounds in Mg−5Li alloys

The XRD results of the as-cast Mg−5Li−*x*Sn alloys are demonstrated in Fig. 4. It reveals that all the Mg−5Li−*x*Sn alloys contain *α*-Mg and Mg_2Sn. $LiOH{\cdot}H_2O$ was observed in the XRD patterns, because Li has high chemical activity and is easy to react with H_2O during the sample preparation. Basically, its existence does not disturb the observation of Mg_2Sn and *α*-Mg.

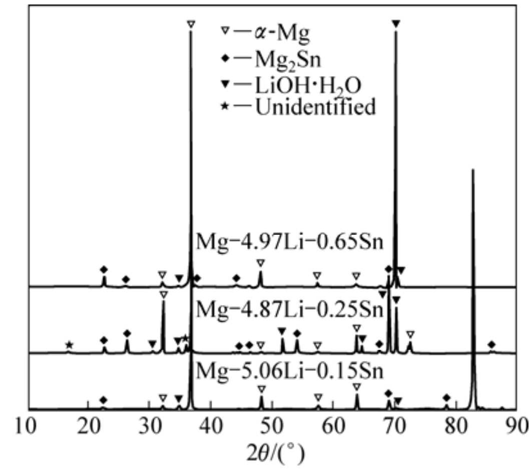

Fig. 4 XRD patterns of as-cast Mg−5Li−*x*Sn alloys

SEM images of the as-cast Mg−5Li−*x*Sn alloys are shown in Fig. 5. As can be observed, most of the second phases are presented as the near net-like shape and distributed at the grain boundary, while some as the granular and inside the grain. Thus, the net-like second phase should be formed during the solidification and the granular ones should be precipitated from *α*-Mg phase. According to both the near net-like and granular phases in the as-cast Mg−5Li−*x*Sn alloys are identified as Mg_2Sn. The volume fraction of Mg_2Sn increases with the increase of Sn addition.

SEM images of the as-extruded Mg−5Li−*x*Sn alloys are shown in Fig. 6 and the EDS analysis is listed in Table 3. Compared to the results in Fig. 5, Mg_2Sn phase with the size of 5−20 μm is changed to granular and no

Table 2 EDS results at different positions in Fig. 5

Position	Molar fraction/%	
	Mg	Sn
A	100	0
B	58.0	42.0
C	95.57	4.43
D	88.80	11.20
E	34.18	65.82
F	33.59	66.41

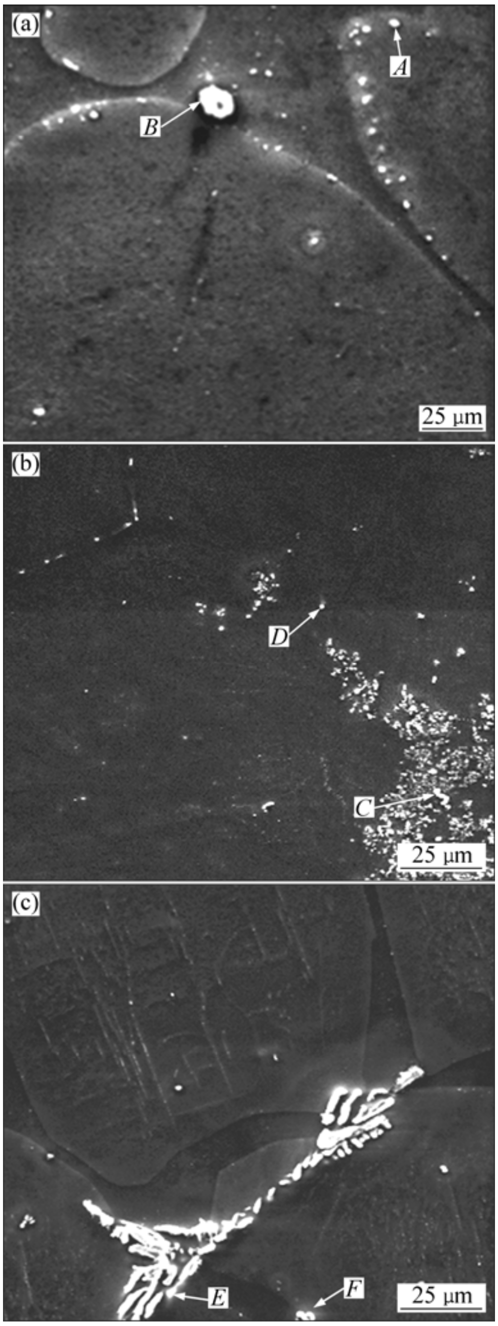

Fig. 5 SEM images of as-cast Mg−5.06Li−0.15Sn (a), Mg−4.87Li−0.25Sn (b) and Mg−4.97Li−0.65Sn (c) alloys

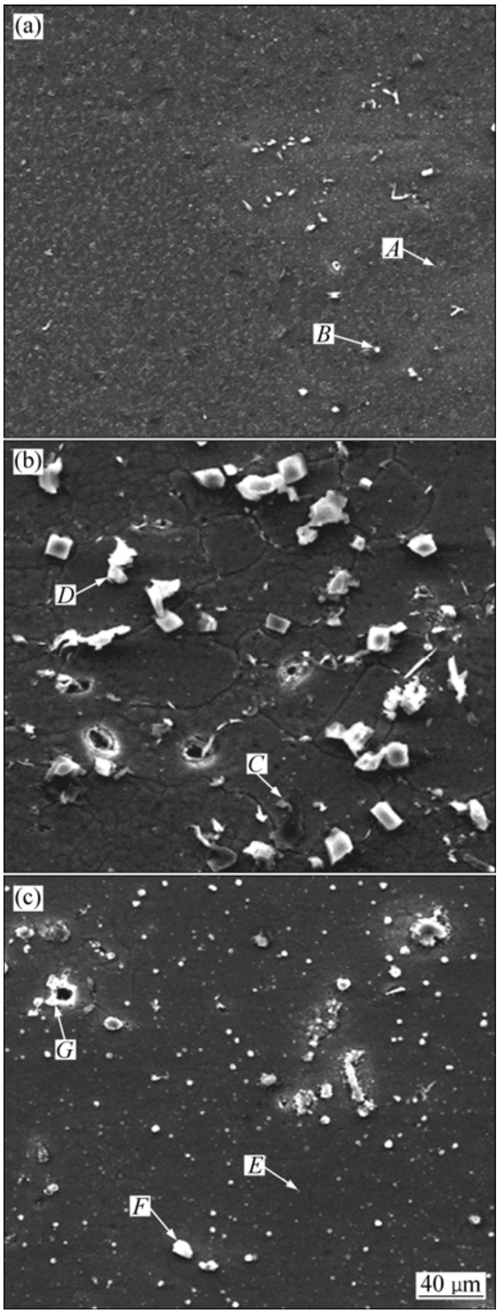

Fig. 6 SEM images of as-extruded Mg−5.06Li−0.15Sn (a), Mg−4.87Li−0.25Sn (b) and Mg−4.97Li−0.65Sn (c) alloys

Table 3 EDS results at different positions in Fig. 6

Position	Molar fraction/%	
	Mg	Sn
A	100	0
B	76.72	23.28
C	100	0
D	93.02	6.98
E	100	0
F	1.78	98.22
G	80.17	19.83

net-like phase is observed, due to the extrusion stress and dynamic recrystallization. Most of them locate inside the grain, and some at the grain boundary.

3.3 Mechanism of grain refinement of Mg−5Li alloys with various Sn additions

The addition of alloying element to metallic materials can reduce the grain size of the matrix, through the growth restriction of grains due to the segregation power of solute elements in the matrix [22−23] and/or through the heterogeneous nucleation of matrix grains [24]. As shown in Fig. 5 and Table 2, there is almost no

Sn dissolved into α-Mg. Meanwhile, The growth restriction parameter of Sn for α-Mg grain is about 1.47 according to Mg−Sn binary phase diagram, which is much less than those of Al, Zn, or Ca for α-Mg grain [25]. Thus, the contribution of Sn to the grain refinement of the as-cast Mg−5Li alloy due to the growth restriction parameter is little. The net-like Mg_2Sn compounds formed during the solidification locate at the grain boundary and can restrain the growth of α-Mg grains to some extent.

During the extrusion, the net-like Mg_2Sn compounds evolve to the granular and may play a key role in the change of microstructure. ZHANG et al [26−27] showed that an intermetallic compound can be the grain refiner for a metal matrix when the crystallography mismatch of the close or near close packed planes between the compound and the metal matrix is less than 10%. According to the crystallographic database and X-ray powder diffraction data [28−29], Mg_2Sn is in body center cubic structure, its three close packed planes are defined as (300), (401), and (330) planes, and those of Mg as $(10\bar{1}1)$, (0002), and $(10\bar{1}0)$ planes. Therefore, there are nine pairs of potential matching planes for Mg and Mg_2Sn. The mismatches of the potential matching planes are defined by the method in Ref. [26]. All the mismatch values are listed in Table 4. There is one matching plane pair between Mg and Mg_2Sn with less than 10% mismatch, which shows that a crystallography orientation relationship exists between Mg and Mg_2Sn, although it needs to be further studied. Therefore, fine uniform Mg_2Sn particles can act as nucleation sites of α-Mg grains during dynamic recrystallization. With the increase of Sn content, the volume fraction of Mg_2Sn particles increases and hence the finer microstructure appears in the as-extruded Mg−5Li−xSn alloys.

Table 4 Mismatch value between α-Mg and Mg_2Sn

Potential matching plane	Mismatch value/%
$(10\bar{1}1)_{Mg}/(300)\tau$	55.0
$(10\bar{1}1)_{Mg}/(401)\tau$	7.7
$(10\bar{1}1)_{Mg}/(330)\tau$	10.4
$(0002)_{Mg}/(300)\tau$	78.9
$(0002)_{Mg}/(401)\tau$	97.0
$(0002)_{Mg}/(330)\tau$	104.0
$(10\bar{1}0)_{Mg}/(300)\tau$	128.4
$(10\bar{1}0)_{Mg}/(401)\tau$	134.9
$(10\bar{1}0)_{Mg}/(330)\tau$	137.4

τ is denoted as Mg_2Sn

4 Conclusions

1) The addition of Sn has obvious grain refinement effect on the as-cast Mg-5Li alloy. The addition of 0.65% (mass fraction) Sn can reduce the grain size of as-cast Mg−5Li alloy from original 567 μm to 345 μm. Meanwhile, the grain size of as-extruded alloys changes from 33 μm to 23 μm when the Sn content ranges from 0.15% to 0.65%.

2) Both α-Mg and Mg_2Sn phases are found in the as-cast and as-extruded Mg−5Li−xSn alloys. Mg_2Sn in the as-cast alloy locates mainly at the grain boundary and exists in near net-like shape and will restrain the growth of grains. After extrusion, Mg_2Sn evolves to granular and distributes more uniformly.

3) Mg_2Sn phase has less than 10% mismatch with α-Mg, and thus Mg_2Sn particles inside the grain can act as nucleation sites for the dynamic recrystallization of α-Mg grains during extrusion.

References

[1] LI J F, ZHENG Z Q, TAO G Y. Ultra-light Mg−Li alloy [J]. Light Alloy Fabrication Technology, 2004, 10: 32−35.

[2] JIANG B, QIU D, ZHANG M X, DING P D, GAO L. A new approach to grain refinement of an Mg−Li−Al cast alloy [J]. Journal of Alloys and Compounds, 2010, 492: 95−98.

[3] AGHION E, BRONFIN B. Magnesium alloys development towards the 21st century [J]. Materials Science Forum, 2000, 350−351: 19−30.

[4] HAFERKAMP H, NIEMEYER M, BOEHEM R, HOLZKAMP U, JASCHIK C, KAESE V. Development, processing and applications range of magnesium lithium alloys [J]. Materials Science Forum, 2000, 350−351: 31−42.

[5] LE Q C, CUI J Z, LI H B, ZHANG X J. Current research development in Mg−Li alloy and its application [J]. Materials Review, 2003, 12: 1−4.

[6] MENG X R, WU R Z, ZHANG M L. Research status of grain refinement strengthening and compound strengthening in super-light Mg−Li alloy [J]. Foundry Technology, 2009, 30: 116−119.

[7] LIU B, ZHANG M L, WU R Z. Effects of Nd on microstructure and mechanical properties of as-cast LA141 alloys [J]. Materials Science and Engineering A, 2008, 487: 347−351.

[8] LUO G X, WU G Q, WANG S J, HUANG Z. Effects of YAl_2 particulates on microstructure and mechanical properties of β-Mg–Li alloy [J]. Materials Science, 2006, 41: 5556−5558.

[9] TROJANOVA Z, DROZD Z, KUDELA S, SZARAZ Z, LUKA P. Strengthening in Mg−Li matrix composites [J]. Composites Science and Technology, 2007, 67: 1965−1973.

[10] JAGER A, LUKA P, GARTNEROVA V, BOHLEN J, KAINER K U. Tensile properties of hot rolled AZ31 Mg alloy sheets at elevated temperatures [J]. Journal of Alloys and Compounds, 2004, 378: 184−187.

[11] MORDIKE B L, EBERT T. Magnesium: Properties—applications—potential [J]. Materials Science and Engineering A, 2001, 302: 37−45.

[12] AL-SAMMAN T. Comparative study of the deformation behavior of hexagonal magnesium-lithium alloys and a conventional magnesium AZ31 alloy [J]. Acta Materialia, 2009, 57: 2229−2242.

[13] MATSUDA A, WAN C C, YANG J M, KAO W H. Rapid solidification processing of the Mg−Li−Sr−Ag alloy [J]. Metallurgical and Materials Transactions A, 1996, 27: 1363−1370.

[14] SONG G S, STAIGER M, KRAL M. Some new characteristics of the strengthening phase in β-phase magnesium−lithium alloys containing

aluminum and beryllium [J]. Materials Science and Engineering A, 2004, 371: 371−376.

[15] SANSCHAGRIN A, TREMBLAY R, ANGERS R, DUBE D. Mechanical properties and microstructure of new magnesium−lithium base alloys [J]. Materials Science and Engineering A, 1996, 1−2: 69−77.

[16] WANG T, ZHANG M L, WU R Z. Microstructure and properties of Mg−8Li−1Al−1Ce alloy [J]. Materials Letters, 2008, 62: 1846−1848.

[17] CHANG T C, WANG J Y, CHU C L, LEE S. Mechanical properties and microstructures of various Mg−Li alloys [J]. Materials Letters, 2006, 60: 3272−3276.

[18] DONG H W, WANG L D, WU Y M, WANG L M. Effect of Y on microstructure and mechanical properties of duplex Mg−7Li alloys [J]. Journal of Alloys and Compounds, 2010, 506: 468−474.

[19] LIU H M, CHEN Y G, TANG Y B, WEI S H, NIU G. The microstructure, tensile properties, and creep behavior of as-cast Mg−(1−10)%Sn alloys [J]. Journal of Alloys and Compounds, 2007, 440: 122−126.

[20] CHEN J H, CHEN Z H, YAN H G, ZHANG F Q, LIAO K. Effects of Sn addition on microstructure and mechanical properties of Mg−Zn−Al alloys [J]. Journal of Alloys and Compounds, 2008, 461: 209−215.

[21] XIANG Q, WU R Z, ZHANG M L. Influence of Sn on microstructure and mechanical properties of Mg−5Li−3Al−2Zn alloys [J]. Journal of Alloys and Compounds, 2009, 477: 832−835.

[22] EASTON M, STJOHN D. Grain refinement of aluminum alloys: Part I. The nucleant and solute paradigms—A review of the literature [J]. Metallurgical and Materials Transactions A, 1999, 30: 1613−1623.

[23] EASTON M, STJOHN D. Grain refinement of aluminum alloys: Part II. Confirmation of, and a mechanism for, the solute paradigm [J]. Metallurgical and Materials Transactions A, 1999, 30: 1625−1633.

[24] FU H M, QIU D, ZHANG M X, WANG H, KELLY P M, TAYLOR J A. The development of a new grain refiner for magnesium alloys using the edge-to-edge model [J]. Journal of Alloys and Compounds, 2008, 456: 390−394.

[25] LEE Y C, DAHLE A K, StJOHN D H. The role of solute in grain refinement of magnesium alloys [J]. Metallurgical and Materials Transaction A, 2000, 31: 2895−2906.

[26] ZHANG M X, KELLY P M, EASTON M A, TAYLOR J A. Crystallographic study of grain refinement in aluminum alloys using the edge-to-edge matching model [J]. Acta Materialia, 2005, 53: 1427−1438.

[27] ZHANG M X, KELLY P M, QIAN M, TAYLOR J A. Crystallography of grain refinement in Mg−Al based alloys [J]. Acta Materialia, 2005, 53: 3261−3271.

[28] VILLARS P, CALVERT L D. Pearson's handbook of crystallographic data for intermetallic phases [M]. Vol. 1. Materials Park, OH: ASM International, 1991.

[29] 2002 JCPDS–International Center For Diffraction Data [S]. PCPDF-WIN v. 2.3.

Sn 对 Mg−5Li 合金铸态和挤压态组织的影响

蒋 斌[1,2]，殷恒梅[1]，杨青山[1,2]，李瑞红[1,2]，潘复生[1,2]

1. 重庆大学 材料科学与工程学院，重庆 400044；
2. 国家镁合金材料工程技术研究中心，重庆 400044

摘 要：在氩气保护气氛下熔炼，得到 Mg−5Li−*x*Sn(*x*=0.15, 0.25 和 0.65，质量分数)系列合金。通过光学显微镜、扫描电镜、X 射线衍射仪和能谱仪分析合金的显微组织。结果表明，Mg−5Li 合金中添加的 Sn 元素可以起到明显的晶粒细化作用，当 Sn 含量从 0.15%增加到 0.65%时，铸态合金的平均晶粒尺寸从 556 μm 细化到 345 μm，相应的挤压态合金的晶粒从 33 μm 减小到 23 μm。近似网状的第二相 Mg_2Sn 分布在铸态合金的晶界上，挤压之后，颗粒状的 Mg_2Sn 主要分布在晶粒内部。这些金属间化合物在挤压动态再结晶中可以作为有效的形核质点，从而起到细化晶粒的作用。

关键词：镁锂合金；晶粒细化；金属间化合物；锡

(Edited by YUAN Sai-qian)